

Proceedings of the 18th National Conference on Superconductivity, Krynica Morska, Poland, October 8–13, 2017

## Magnetic Properties of $Y_{11}Co_4In_9$

S. BARAN<sup>a</sup>, J. PRZEWOŹNIK<sup>b</sup>, YA. KALYCHAK<sup>c</sup>, YU. TYVANCHUK<sup>c</sup> AND A. SZYTUŁA<sup>a,\*</sup>

<sup>a</sup>M. Smoluchowski Institute of Physics, Jagiellonian University, S. Łojasiewicza 11, 30-348 Kraków, Poland

<sup>b</sup>AGH University of Science and Technology, Faculty of Physics and Applied Computer Science,

Department of Solid State Physics, al. A. Mickiewicza 30, 30-059 Kraków, Poland

<sup>c</sup>Analytical Chemistry Department, Ivan Franko National University of Lviv,

Kyryla and Mephodiya 6, 79005 Lviv, Ukraine

The intermetallic  $Y_{11}Co_4In_9$  compound has been synthesized, and its crystal structure and magnetic properties are reported. Powder X-ray diffraction measurements at room temperature and the Rietveld analysis show that the compound crystallizes in an orthorhombic  $Nd_{11}Pd_4In_9$  structure with  $Cmmm$  space group. Temperature dependence of the AC magnetic susceptibility indicates the broad maximum at 10 K while DC data give in this temperature separation on zero field cooled and field cooled susceptibility with the negative value of zero field cooled data. Above 10 K the DC magnetic susceptibility does not obey the Curie–Weiss law. The magnetization curve at 1.9 K does not show saturation at  $H = 90$  kOe, with the small value of the magnetic moment equal to  $0.14 \mu_B/f.u.$

DOI: [10.12693/APhysPolA.135.36](https://doi.org/10.12693/APhysPolA.135.36)

PACS/topics: 75.30.Cr, 75.30.Kz

### 1. Introduction

Compounds of rare earths with transition metals and indium show interesting physical properties and became the object of intensive investigations [1]. Compounds with the composition 11:4:9 and Ni as the transition metal form specially interesting group. These compounds crystallize in the orthorhombic  $Nd_{11}Pd_4In_9$ -type crystal structure (space group  $Cmmm$ ,  $Z = 2$ ) [2]. The results of the magnetic and neutron diffraction measurements indicate complex magnetic properties of  $R_{11}Ni_4In_9$  compounds [3–7]. Also the compounds with Co have the similar crystal structure [8].

This work reports the results of investigations of the crystal structure and magnetic properties as well as electrical resistivity of  $Y_{11}Co_4In_9$  compound.

### 2. Experimental procedures

A sample of total weight of  $\approx 1.5$  g was obtained by a standard melting procedure: the amounts of the elements with the nominal composition of  $Y_{11}Co_4In_9$  were arc-melted under a pure argon atmosphere on a water cooled copper hearth with a tungsten electrode and titanium serving as a getter. Ingots of yttrium of the purity not lower than 99.95 wt%, cobalt 99.91 wt% and indium 99.99 wt% were used as the starting materials. Yttrium pieces were first arc-melted to small button. The pre-melting procedure of yttrium strongly reduces shattering during the subsequent reaction with cobalt and indium.

The resulting button was turned over and re-melted twice in order to ensure homogeneity. The button was sealed in an evacuated silica tube and annealed at 870 K for 2 months.

X-ray powder diffraction pattern for determining the crystal structure was collected on a PANalytical X'Pert Pro diffractometer (Cu  $K_{\alpha 1}$  radiation). Obtained result was analyzed by the FullProf program [9].

The DC magnetic susceptibility was measured as a function of temperature (in the range 1.9–200 K) and applied magnetic fields (0–90 kOe) using a Physical Property Measurement System Quantum Design (PPMS QD). Resistivity measurements were recorded using a four probe method between 2 at 300 K and zero magnetic field.

The AC magnetic susceptibility  $\chi_{ac} = \chi' + i\chi''$ , where  $\chi'$  is a real and  $\chi''$  is an imaginary component, was measured versus frequency between 500 Hz and 10 kHz with magnetic field amplitude  $H_{AC}$  equal to 2 Oe within temperature range 2–20 K.

### 3. Results

#### 3.1. Crystal structure

The X-ray powder diffraction pattern  $Y_{11}Co_4In_9$  collected at room temperature is shown in Fig. 1. The diffraction data confirm an orthorhombic crystal structure of the  $Nd_{11}Pd_4In_9$  type (space group  $Cmmm$ ). The determined values of lattice parameters are:  $a = 1.4386(2)$  nm,  $b = 2.1576(4)$  nm,  $c = 0.36285(8)$  nm,  $V = 1.1262(4)$  nm<sup>3</sup>. The refined values of atomic coordinates together with reliability factors are listed in Table I.

\*corresponding author; e-mail: [andrzej.sztytula@uj.edu.pl](mailto:andrzej.sztytula@uj.edu.pl)

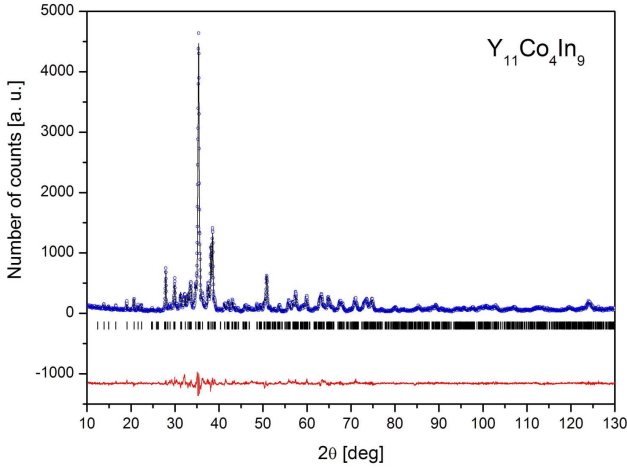


Fig. 1. X-ray diffraction pattern of  $Y_{11}Co_4In_9$  collected at room temperature. The experimental points are represented by small circles while the solid black lines refer to calculated pattern and a difference between the experimental and calculated intensities red line (at the bottom of diagram). The vertical bars indicate the positions of the Bragg reflections.

TABLE I

Refined structural parameters for  $Y_{11}Co_4In_9$  at room temperature ( $Nd_{11}Pd_4In_9$  type structure, space group  $Cmmm$ ). Preferred orientation: direction and parameter  $[001] 0.79(1)$ ,  $R_F = 3.76\%$ ,  $R_{Bragg} = 6.72\%$ ,  $\chi^2 = 2.35$ )

Atom	Wyckoff site	$x$	$y$	$z$
Y1	$8p$	0.2475(8)	0.1683(8)	0
Y2	$4i$	0	0.1613(8)	0
Y3	$4i$	0	0.3748(8)	0
Y4	$4g$	0.3123(13)	0	0
Y5	$2a$	0	0	0
Co	$8q$	0.3483(16)	0.1012(13)	1/2
In1	$8q$	0.1036(5)	0.2644(5)	1/2
In2	$8q$	0.1493(8)	0.0717(4)	1/2
In3	$2c$	1/2	0	1/2

### 3.2. Magnetic AC and DC susceptibility data

Figure 2 reports temperature dependence of the real  $\chi'$  and imaginary  $\chi''$  component of AC magnetic susceptibility data collected at a number of frequencies between 500 Hz and 10 kHz in external magnetic field 2 Oe. In  $\chi'(T)$  and  $\chi''(T)$  dependences a broad maximum at 10 K in  $\chi'(T)$  and 12 K in  $\chi''(T)$  is shown. The positions of those maxima do not change with frequency.

The temperature dependence of the DC magnetic susceptibility at  $H = 1$  kOe (see Fig. 3) above 100 K is nearly constant and changes from  $5 \times 10^{-3}$  emu/mol at 100 K to  $3.6 \times 10^{-3}$  emu/mol at 400 K. With decrease of temperature below 100 K it increases first slowly and then below 15 K quickly, reaching maximum at 3.5 K.

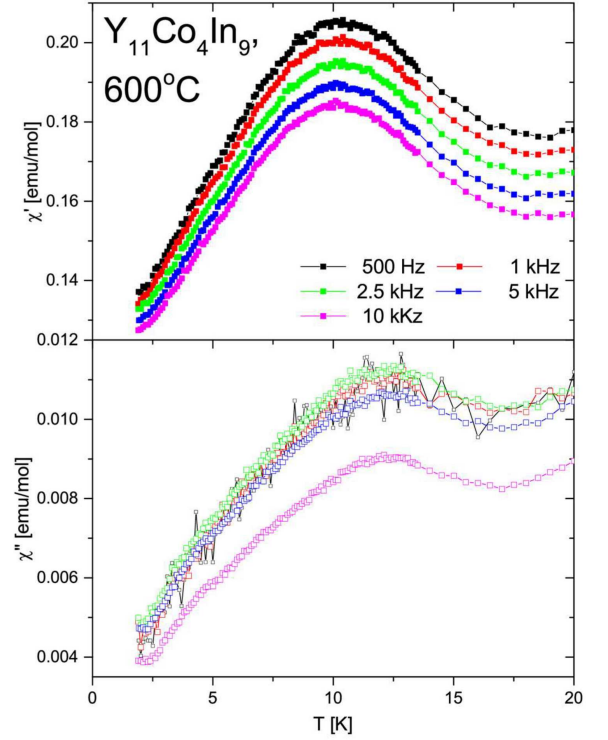


Fig. 2. Temperature dependence of the real  $\chi'$  and imaginary  $\chi''$  components of AC magnetic susceptibility of  $Y_{11}Co_4In_9$  measured at temperature range 2–20 K and frequency between 500 Hz and 10 kHz in external magnetic field 2 Oe.

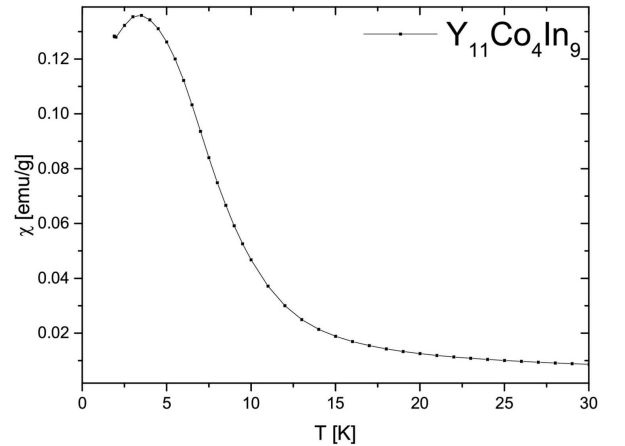


Fig. 3. Temperature dependence of the DC FC magnetic susceptibility of  $Y_{11}Co_4In_9$  at  $H = 1$  kOe.

Dependences of zero field cooled (ZFC) and field cooled (FC) curves at  $H = 50$  Oe are very different (see Fig. 4). The FC susceptibility is positive and increases with decrease of temperatures. Dependences of the ZFC data are characterized by a maximum near  $T_m = 10$  K for  $H = 50$  Oe and next a quick decrease and change the sign from positive to negative at  $T_0$  equal to 8.6 K. The values of both  $T_m$  and  $T_0$  decrease with the increase of the external magnetic field (see inset in Fig. 4).

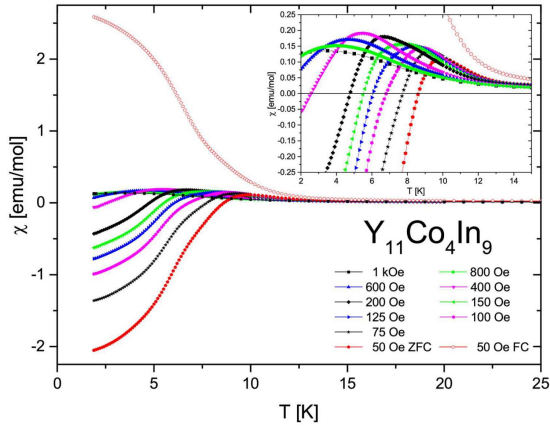


Fig. 4. Temperature dependence of the FC and ZFC magnetic susceptibility of  $Y_{11}Co_4In_9$  at  $H = 50$  Oe. ZFC curves were measured at different magnetic field between 50 Oe and 1 kOe. Inset shows the data in temperature range 2–20 K and small values of magnetic susceptibility.

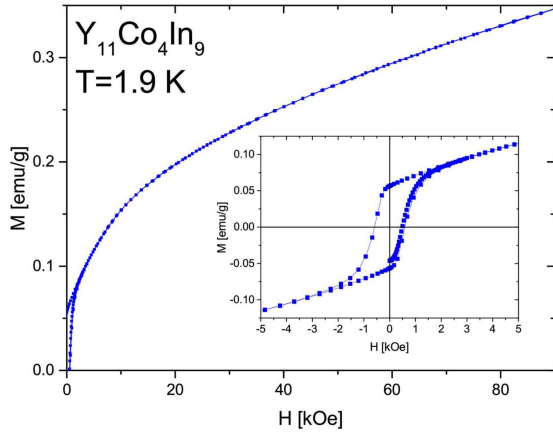


Fig. 5. Magnetization curve of  $Y_{11}Co_4In_9$  at temperature 1.9 K and in external magnetic field up to 90 kOe. Inset shows the hysteresis loop.

Figure 5 shows the magnetization curve for  $Y_{11}Co_4In_9$  measured at 1.9 K and at applied magnetic fields up to 90 kOe. Magnetization slowly increases with increase of magnetic field and is equal to  $0.14 \mu_B/f.u.$  at  $H = 90$  kOe. Inset in Fig. 5 shows the hysteresis loop which is similar to that observed in  $Y_9Co_7$  (see inset in Fig. 1 in Ref. [10]).

### 3.3. Electrical resistivity

Temperature dependence of the electrical resistivity of  $Y_{11}Co_4In_9$  is shown in Fig. 6. Similar dependence of the electrical resistivity is observed in isostructural  $Y_{11}Ni_4In_9$ . Both compounds are characterized by the large values of remanence resistivity. With increase of the temperature, electrical resistivity increases as  $T^n$  where  $n = 3$  for the temperature range 2–30 K and  $n = 0.54$  for 30–300 K.

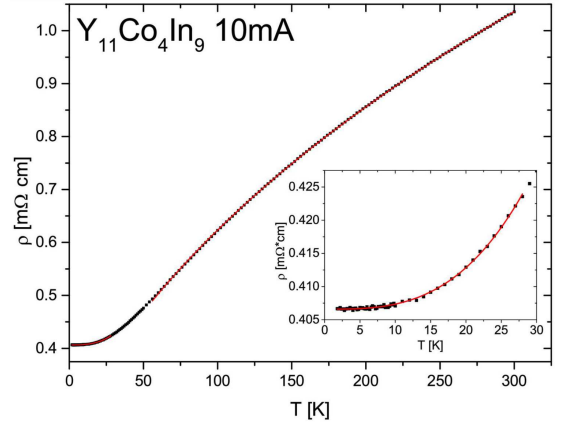


Fig. 6. Electrical resistivity of  $Y_{11}Co_4In_9$  between 2 and 300 K. Inset shows low temperature data.

The value of a residual resistivity ratio (RRR)  $\rho_{300 K}/\rho_0$  is equal to 2.5 and is close to values observed in the isostructural  $R_{11}Ni_4In_9$  ( $R = Gd, Tb, Dy, Y$ ) compounds. For these compounds the electrical resistivity was measured on the oriented fibers parallel (along  $c$ -axis) and orthogonal (in  $a$ - $b$  plane) to the electrical current direction. The value of RRR are equal to 6.7 ( $p =$  parallel) and 4.5 ( $o =$  orthogonal) for  $R = Gd$  [6], 6.0 ( $p$ ) and 3.9 ( $o$ ) for  $R = Tb$ , 4.0 ( $p$ ) and 4.25 ( $o$ ) for  $R = Dy$  and 4.0 ( $p$ ) and 2.9 ( $o$ ) for  $R = Y$  [5]. The low values of RRR are connected with the large values of  $\rho_0$ , thereby indicating the substantial amount of atomic disorder, complex crystal structure and also the existence of structural defect and the grain boundary effects in investigated polycrystalline samples.

## 4. Discussion and summary

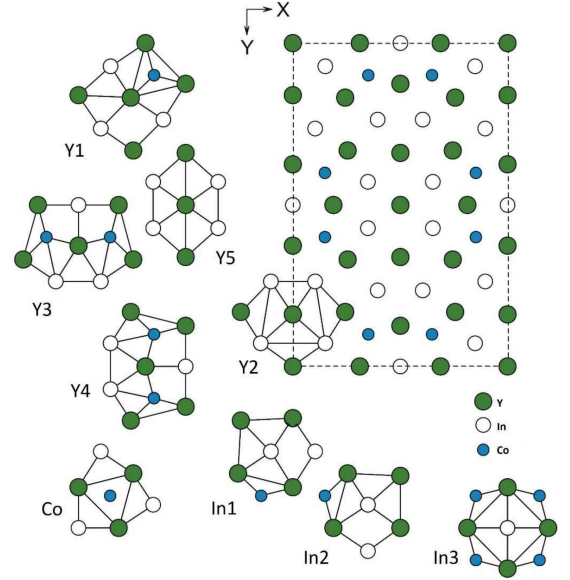
The investigated  $Y_{11}Co_4In_9$  compound crystallizes in the orthorhombic  $Nd_{11}Pd_4In_9$  type structure with large values of  $a$  and  $b$  lattice parameters and small  $c$  one. The crystal structure is a two-layered structure along the short unit cell  $c$ -axis. A projection of the unit cell on the  $a$ - $b$  plane and the corresponding polyhedra of the atoms are shown in Fig. 7. The Y atoms occupy five sites, Co — one site, and In — three sites. Determined values of interatomic distances (see Table II) indicate values smaller than the sum of atomic radius equal to: Co — 0.125 nm, Y — 0.180 nm and In — 0.166 nm between Co and Y and In atoms. The small Co–Y interatomic distances indicate the hybridization of Co  $3d$  and Y  $4d$  states.

Presented magnetic data indicate the complex properties of this compound. The maximum at  $\chi'(T)$  indicates the short range magnetic clustering. Comparison of low temperatures DC data for  $Y_{11}Co_4In_9$  with those for isostructural  $Y_{11}Ni_4In_9$ , which is the Pauli paramagnet [5], indicates that the magnetic moment is connected with the Co atoms. The small value of moment determined from the magnetization equals  $0.14 \mu_B/f.u.$  ( $\approx 0.04 \mu_B/Co$  atom) indicates the itinerant character of those properties.

Interatomic distances and coordination number of atoms of  $Y_{11}Co_4In_9$ .

TABLE II

Atom / CN		To atom	$d$ [nm]
Y1 CN = 14	2x	Co	0.27368
	2x	In2	0.31035
	2x	In1	0.31607
	2x	In1	0.34458
	1x	Y1	0.35262
	1x	Y2	0.35637
	2x	Y1	0.36285
	1x	Y4	0.37489
1x	Y3	0.37496	
Y2 CN = 13	4x	In1	0.32339
	4x	In2	0.34121
	1x	Y5	0.34801
	2x	Y1	0.35637
	2x	Y2	0.36285
Y3 CN = 16	4x	Co	0.28848
	2x	In3	0.32540
	4x	In1	0.33451
	2x	Y3	0.36285
	2x	Y1	0.37496
	2x	Y4	0.38194
Y4 CN = 16	4x	Co	0.28857
	2x	In3	0.32531
	4x	In2	0.33440
	2x	Y4	0.36285
	2x	Y1	0.37489
	2x	Y3	0.38194
Y5 CN = 12	8x	In2	0.32089
	2x	Y2	0.34801
	2x	Y5	0.36285
Co CN = 9	2x	Y1	0.27368
	2x	Y3	0.28848
	2x	Y4	0.28857
	1x	In2	0.29327
	1x	In1	0.29818
	1x	In3	0.30871
In1 CN = 12	1x	In1	0.29807
	1x	Co	0.29818
	2x	Y1	0.31607
	2x	Y2	0.32339
	2x	Y3	0.33451
	2x	Y1	0.34458
	2x	In1	0.36285
In2 CN = 12	1x	Co	0.29327
	1x	In2	0.30935
	2x	Y1	0.31035
	2x	Y5	0.32089
	2x	Y4	0.33440
	2x	Y2	0.34121
	2x	In2	0.36285
In3 CN = 14	4x	Co	0.30871
	4x	Y4	0.32531
	4x	Y3	0.32540
	2x	In3	0.36285

Fig. 7. Projection of the unit cell of  $Y_{11}Co_4In_9$  on the  $a$ - $b$  plane and coordination polyhedra of atoms.

Observed negative values of the low temperature ZFC magnetization is a new surprise. Similar effect is observed in a large number of intermetallics characterized by the complex crystal structure [11].

The negative values of the magnetic susceptibility of the ZFC measured at low temperatures shown in Fig. 4, is produced by the change in the orbital motion of electrons due to the applied magnetic field. The direction of the induced magnetic moment is opposite to the direction of the applied field, which results in a negative magnetic susceptibility, associated with the diamagnetic term  $\chi_{DC}$  [12].

The magnetic data obtained in this work are similar to those for  $Y_9Co_7$  [10]. In both compounds at low temperatures the magnetization with the very small values of the Co magnetic moments is observed. The data for  $Y_9Co_7$  indicate that the observed ferromagnetic properties below 4.5 K have a weak itinerant character. In  $Y_{11}Co_4In_9$  below 20 K the separation of ZFC and FC susceptibility indicate the short-range order. The decrease of temperatures corresponding to the maximum with increase of the magnetic field from 10 K at 50 Oe to 3.5 K at 1 kOe indicates the antiferromagnetic character of these ordering.

Investigated compound is included in the series of Y-Co compounds whose magnetic behaviour is connected with the band structure [13].

### Acknowledgments

The research was carried out with the equipment purchased thanks to the financial support of the European Regional Development Fund in the framework of the Polish Innovation Economy Operational Program (contract no. POIG.02.01.000-023/08). Thanks are due to Dr. Bogusław Penc for the preparation of the graphical part of this work.

## References

- [1] Ya.M. Kalychak, V.I. Zaremba, R. Pottgen, M. Lukachuk, R.-D. Hofmann, in: *Handbook on Physics and Chemistry of Rare Earths*, Eds. K.S. Gschneidner Jr., V.K. Pecharsky, J.-C. Banzil, Elsevier, Amsterdam 2005, Vol. 34, p. 1.
- [2] L. Sojka, M. Manyako, R. Černý, M. Ivanyk, B. Belan, R. Gladyshevskii, Y. Kalychak, *Intermetallics* **16**, 625 (2008).
- [3] Yu. Tyvanchuk, S. Baran, R. Duraj, Ya.M. Kalychak, J. Przewoźnik, A. Szytuła, *J. Alloys Comp.* **587**, 573 (2014).
- [4] A. Szytuła, S. Baran, J. Przewoźnik, Yu. Tyvanchuk, Ya. Kalychak, *J. Alloys Comp.* **601**, 238 (2014).
- [5] A. Provino, K.A. Gschneidner Jr., S.K. Dhar, C. Ferdeghini, Y. Mudryk, P. Manfrinetti, D. Paudyal, V.K. Pecharsky, *Acta Mater.* **91**, 128 (2015).
- [6] A. Provino, P. Manfrinetti, K.A. Gschneidner Jr., S.K. Dhar, D.L. Schlagel, T.A. Lograsso, G.J. Miller, S. Thimmaiah, Hui Wang, A.M. Russell, A. Becker, Y. Mudryk, *Acta Mater.* **73**, 27 (2014).
- [7] C. Ritter, P. Manfrinetti, V.K. Pecharsky, K.A. Gschneidner Jr., S.K. Dhar, *J. Phys. Condens. Matter* **27**, 476001 (2015).
- [8] M. Dzevenko, A. Hamyk, Yu. Tyvanchuk, Ya. Kalychak, *Centr. Eur. J. Chem.* **11**, 604 (2013).
- [9] J. Rodriguez-Carvajal, *Physica B* **192**, 55 (1993).
- [10] Ł. Bochenek, K. Rogacki, A. Kołodziejczyk, T. Cichorek, *Phys. Rev. B* **91**, 235314 (2015).
- [11] W. Suski, *Mater. Sci.-Poland* **25**, 333 (2007).
- [12] J.H. Van Vleck, *The Theory of Electric and Magnetic Susceptibilities*, Oxford University Press, 1991.
- [13] B.R. Coles, A.K. Chhabra, *J. Magn. Magn. Mater.* **54–57**, 1039 (1986).